Reducing anisotropy of topological operators for grayscale images

Francisco Nivando Bezerra and Michel Couprie

Laboratoire A^{2}SI, ESIEE Cité Descartes B.P. 99
93162 Noisy-Le-Grand Cedex France

ABSTRACT

The cross-section topology is a framework that extends the notions of digital topology to the case of grayscale images. In this framework, the use of 4- and 8-connectedness induces geometric constraints in topological operators such as thinning operators. We propose a general method to obtain better results by reducing the anisotropy of such operators. We illustrate the method with an application to the segmentation of human head MRI images.

Keywords: digital topology, cross-section topology, destructible point, anisotropy, grayscale thinning, filtering, segmentation.

1. INTRODUCTION

A grayscale image can be seen as a topographic relief where the gray-level of each pixel represents its altitude. Topographic features such as crests, peaks, saddles and valleys can be used to describe the topology of the image. The cross-section topology approach is based on the decomposition of a map into its different sections[1,2]: let F be a map from $\mathcal{Z}^2$ into $\mathcal{Z}$, the section of F at level k is the set F_k of points x in $\mathcal{Z}^2$ such that $F(x) \geq k$. Following this approach, a transformation is homotopic, i.e. preserves the topology of F, if it preserves the topology, in the binary sense, of every section F_k. Unessential points to the topology can have their gray-level changed while preserving the topology. Such points are called destructible (if they can be lowered) or constructible (if they can be raised). We can, for example, iteratively extend the valleys by lowering the altitude of destructible points until crests and mountains have been reduced to thin lines and peaks.[2–5] These features have great importance in shape description. It is also possible to limit the extent of this operation, in order to discriminate objects that have a width inferior to a given value: only those objects can be reduced to thin lines and can thus be detected and analyzed. This approach leads to new filtering and segmentation schemes (see[4,5] and section 7 of this paper).

It can be seen that using existing approaches, such a thinning process is characterized by a breadth-first propagation implicitly guided by the distance d_8, intrinsically related to the discrete nature of digital images. As this distance measure is anisotropic, i.e. is not rotation invariant, the result of such transformations is sensitive to the orientation of the original object. For binary images, alternative approaches use a distance map to find the centers of maximal disks inscribed in the object to be thinned. Using an exact or approximate euclidean distance map[6–8] we may obtain less anisotropic skeletons. This approach cannot be directly extended to grayscale images because it is impossible to build a distance map of a grayscale image.

We introduce an original method for reducing anisotropy of grayscale image thinning operators. During the thinning process, when a destructible point is lowered, it takes the same grayscale value as one of its 8-neighbors. In order to control the propagation of these grayscale values, we associate to each point x a pointer $T(x)$ which indicates the spatial origin of the grayscale value of the point x. Initially, we set $T(x) := x$ for all x, and at each step of the thinning process, when a destructible point x is lowered down to the value of one of its neighbors y, we also execute $T(x) := T(y)$. This allows us to control the spatial extent of the process by subordinating the modification of a destructible point x to the following condition: if x may be lowered down to the value of its neighbor y, it will indeed be lowered down to $F(y)$ only if the distance between x and $T(y)$ is smaller than a certain threshold d_{max}.

The important point is that the distance used to control the thinning process can be chosen ad libitum. For anisotropy reduction purposes, the euclidean distance is used.

Sections 2 and 3 recall the main concepts and definitions of digital topology for binary images[9] and grayscale images,[2] respectively. In section 4, we present some image processing algorithms based on topology. Improved

Correspondence: E-mail: bezerraf,coupriem@esiee.fr; Web: http://www.esiee.fr/a2si

versions of these algorithms providing centered skeletons, as well as the anisotropic behavior of these algorithms are discussed in section 5. Section 6 discusses the problem of reducing anisotropy and introduces our new method. Section 7 exemplifies the use of reduced anisotropy operators with a segmentation of the external layer of human head MRI. Section 8 summarizes and concludes this work.

2. TOPOLOGY OF BINARY IMAGES

In this section, we recall some basic notions of digital topology for binary images.[9] We denote by $\mathcal{Z}$ the set of relative integers. A point $x \in \mathcal{Z}^2$ is defined by (x_1, x_2) with $x_i \in \mathcal{Z}$. We consider the two neighborhoods relations Γ_4 and Γ_8 defined for each point $x \in \mathcal{Z}^2$ by: $\Gamma_4(x) = \{y \in \mathcal{Z}^2; |y_1 - x_1| + |y_2 - x_2| \leq 1\}$, $\Gamma_8(x) = \{y \in \mathcal{Z}^2; \max(|y_1 - x_1|, |y_2 - x_2|) \leq 1\}$. In the following, we will denote by n a number such that $n = 4$ or $n = 8$. We define $\Gamma_n^*(x) = \Gamma_n(x) \setminus \{x\}$. The point $y \in \mathcal{Z}^2$ is *n-adjacent* to $x \in \mathcal{Z}^2$ if $y \in \Gamma_n^*(x)$. An *n-path* is a sequence of points $x_0 \ldots x_k$ with x_i n-adjacent to x_{i-1} for $i = 1 \ldots k$. The distances d_4 and d_8 between x and y are defined by $d_4(x, y) = |x_1 - y_1| + |x_2 - y_2|$, $d_8(x, y) = \max(|x_1 - y_1|, |x_2 - y_2|)$.

Let $X \subset \mathcal{Z}^2$, we denote by $\overline{X}$ the complementary set of X. We say that two points x, y of $\mathcal{Z}^2$ are *n-connected in X* if there is an n-path in X between these two points. This defines an equivalence relation. The equivalence classes for this relation are the *n-connected components* of X. An object $X \subset \mathcal{Z}^2$ is said to be *n-connected* if it consists in exactly one n-connected component. The set composed of all n-connected components of X n-adjacent to a point x is denoted by $C_n[x, X]$. In order to have a correspondence between the topology of X and the topology of $\overline{X}$, we have to consider two different kinds of adjacency for X and $\overline{X}$: if we use the n-adjacency for X, we must use the $\overline{n}$-adjacency for $\overline{X}$, with $(n, \overline{n}) = (8, 4)$ or $(4, 8)$. Let $X \subset \mathcal{Z}^2$ and $x \in \mathcal{Z}^2$, the two *connectivity numbers* are defined as follows ($\#X$ stands for the cardinal of X):

$$T(x, X) = \#C_n[x, \Gamma_8^*(x) \cap X];\ \overline{T}(x, X) = \#C_{\overline{n}}[x, \Gamma_8^*(x) \cap \overline{X}].$$

We say that $x \in X$ is an *isolated point* if $T(x, X) = 0$, a *border point* if $\overline{T}(x, X) > 0$, an *interior point* if $\overline{T}(x, X) = 0$. The point $x \in X$ is *simple (for X)* if there is a bijection between the n-components of X and those of $X \setminus \{x\}$ and also between the $\overline{n}$-components of $\overline{X}$ and those of $\overline{X} \cup \{x\}$. The following property allows to locally characterize simple points[9,10]: $x \in \mathcal{Z}^2$ is simple for $X \subset \mathcal{Z}^2 \Leftrightarrow T(x, X) = 1$ and $\overline{T}(x, X) = 1$. Let $X, Y \subset \mathcal{Z}^2$. The set Y is *lower homotopic to X* if $Y = X$ or Y may be obtained from X by iterative deletion of simple points. The set Y is *upper homotopic to X* if $Y = X$ or Y may be obtained from X by iterative addition of simple points. Two sets X and Y are *homotopic* if $Y = X$ or Y may be obtained from X by iterative deletions or additions of simple points.

3. BASIC NOTIONS FOR GRAYSCALE IMAGES

In this section, we recall the basic definitions and properties of the cross-section topology.[2] First, we recall some basic notions for grayscale images. A 2D grayscale image may is a map $F : \mathcal{Z}^2 \mapsto \mathcal{Z}$ to $\mathcal{Z}$. For each point $x \in \mathcal{Z}^2$, $F(x)$ is the (gray-level) value of x. We denote by $\mathcal{F}$ the set composed of all maps from $\mathcal{Z}^2$ to $\mathcal{Z}$.

Let $F \in \mathcal{F}$ and $k \in \mathcal{Z}$, the *section of F at the level k* is the set F_k composed of all points $x \in \mathcal{Z}^2$ such that $F(x) \geq k$. Observe that a section is a set of points, i.e. a binary image. As for the binary case, if we use the n-adjacency for the sections F_k of F, we must use the $\overline{n}$-adjacency for the complementary sets $\overline{F_k}$, $(n, \overline{n}) = (8, 4)$ or $(4, 8)$. Let us consider the map $-F$, called the *complementary map* of F. We note that the complementary sets of the sections of F are sections of $-F$. When not explicitly specified, in the examples and figures of this paper, we will choose $n = 8$ for the sections of F, thus we must use $\overline{n} = 4$ for the sections of $-F$. A non-empty connected component X of a section F_k of F is a *(regional) maximum for F* if $X \cap F_{k+1} = \emptyset$. A set $X \subset \mathcal{Z}^2$ is a *(regional) minimum for F* if it is a regional maximum for $-F$.

Intuitively, a transformation on F is said to be topology preserving if the topology of all the sections of F is preserved. Thus, the cross-section topology of maps (i.e. of grayscale images) may be directly derived from the topology of binary images. The following notions generalize the notion of simple point to grayscale images.

Let $F \in \mathcal{F}$, the point $x \in \mathcal{Z}^2$ is *destructible (for F)* if x is simple for F_k, with $k = F(x)$. The point $x \in \mathcal{Z}^2$ is *constructible (for F)* if x is destructible for $-F$.

We see that the gray-level value of a destructible (respectively constructible) point can be lowered (respectively raised) by 1 while preserving the topology of F. For example in Fig. 1 (a), the point at gray-level 8 is both

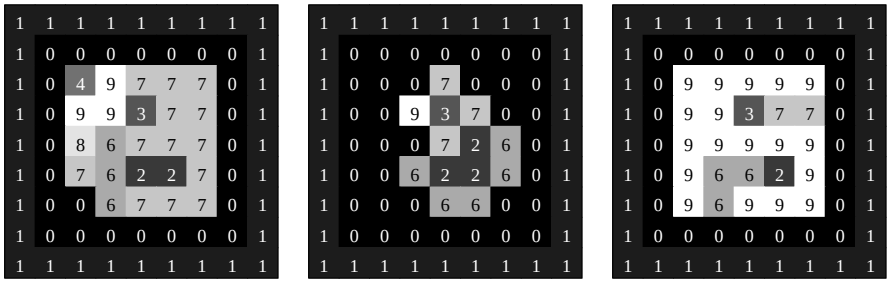

Figure 1. *Homotopic kernels. (a): original image; (b): a lower homotopic kernel (ultimate skeleton) of (a); (c): an upper homotopic kernel of (a).*

destructible and constructible; the two points at gray-level 2 are constructible, but only one of them may be raised because, afterwards, the other one should become non-constructible.

Let $F \in \mathcal{F}$ and $G \in \mathcal{F}$. The map G is *lower homotopic to* F if $G = F$ or G may be obtained from F by iteratively selecting a destructible point and lowering its value by 1. The map G is *upper homotopic to* F if $G = F$ or G may be obtained from F by iteratively selecting a constructible point and raising its value by 1. The maps G and F are *homotopic* if $G = F$ or G may be obtained from F by iteratively selecting a destructible (resp. constructible) point and lowering (resp. raising) its value by 1.

In Fig. 1, (b) is lower homotopic to (a) and (c) is upper homotopic to (a). Note that F and G are homotopic if and only if every section F_k of F is homotopic, in the binary sense, to the corresponding section G_k of G.

Let $F \in \mathcal{F}$ and $x \in \mathcal{Z}^2$. We define the four neighborhoods:

$$\begin{array}{rclrcl} \Gamma^{++}(x,F) & = & \{y \in \Gamma_8^*(x); F(y) > F(x)\}; & \Gamma^{+}(x,F) & = & \{y \in \Gamma_8^*(x); F(y) \geq F(x)\}; \\ \Gamma^{--}(x,F) & = & \{y \in \Gamma_8^*(x); F(y) < F(x)\}; & \Gamma^{-}(x,F) & = & \{y \in \Gamma_8^*(x); F(y) \leq F(x)\}. \end{array}$$

We define the values:

$$\alpha^-(x,F) = \begin{cases} \max\{F(y); y \in \Gamma^{--}(x,F)\}, & \text{if } \Gamma^{--}(x,F) \neq \emptyset, \\ F(x) & \text{otherwise;} \end{cases}$$

$$\alpha^+(x,F) = \begin{cases} \min\{F(y); y \in \Gamma^{++}(x,F)\}, & \text{if } \Gamma^{++}(x,F) \neq \emptyset, \\ F(x) & \text{otherwise.} \end{cases}$$

For a point x, we define the value $\delta^-(x,F)$ which is the minimal value down to which the point x may be lowered without changing the topology of the sections. So, for a destructible point we have $\delta^-(x,F) < F(x)$, and for a non-destructible point we have $\delta^-(x,F) = F(x)$. The value $\delta^+(x,F)$ is defined in a dual way.

It is easy to prove that lowering a destructible point x down to the value $\alpha^-(x,F)$ is an homotopic transformation, i.e. that $\delta^-(x,F) \leq \alpha^-(x,F)$; and in a dual way, that $\delta^+(x,F) \geq \alpha^+(x,F)$. For example in Fig. 1 (a), the point at gray-level 9 in the third row can be lowered down to 7 without changing the cross-section topology, then down to 4, and finally down to 0. This property, in addition to the local characterization of destructible and constructible points which will be presented in the next paragraphs, allows us to design efficient algorithms to compute topological transforms.

We define the four *connectivity numbers*:

$$\begin{array}{rclrcl} T^{++}(x,F) & = & \#C_n[x, \Gamma^{++}(x,F)]; & T^{+}(x,F) & = & \#C_n[x, \Gamma^{+}(x,F)]; \\ T^{--}(x,F) & = & \#C_{\overline{n}}[x, \Gamma^{--}(x,F)]; & T^{-}(x,F) & = & \#C_{\overline{n}}[x, \Gamma^{-}(x,F)]. \end{array}$$

When there is no confusion, we write: $T^{++} = T^{++}(x,F)$, $T^{+} = T^{+}(x,F)$, $T^{--} = T^{--}(x,F)$, $T^{-} = T^{-}(x,F)$.

The following property may be directly derived from the above definitions and from the characterization of simple points in binary images. It shows that the connectivity numbers allow to locally characterize destructible and

constructible points. Let $F \in \mathcal{F}$ and $x \in \mathcal{Z}^2$. x is destructible for $F \Leftrightarrow T^+ = 1$ and $T^{--} = 1$; x is constructible for $F \Leftrightarrow T^- = 1$ and $T^{++} = 1$. Furthermore, the connectivity numbers allow a classification of the topological characteristics of a point: x is a *peak* if $T^+ = 0$; x is *minimal* if $T^{--} = 0$; x is *k-divergent* if $T^{--} = k$ with $k > 1$; x is a *well* if $T^- = 0$; x is *maximal* if $T^{++} = 0$; x is *k-convergent* if $T^{++} = k$ with $k > 1$; x is a *lower point* if it is not maximal; x is an *upper point* if it is not minimal; x is an *interior point* if it is both minimal and maximal; x is a *simple side* if it is both destructible and constructible; x is a *saddle point* if it is both convergent and divergent.

By considering all the possible values of the four connectivity numbers it may be seen[2] that, for $F \in \mathcal{F}$, a point $x \in \mathcal{Z}^2$ corresponds necessarily to one and only one of the following types: 1) a peak; 2) a well; 3) an interior point; 4) a minimal constructible point; 5) a maximal destructible point; 6) a minimal convergent point; 7) a maximal divergent point; 8) a simple side; 9) a destructible convergent point; 10) a constructible divergent point; 11) a saddle point.

4. TOPOLOGICAL OPERATORS

Several grayscale image processing operators based on the cross-section topology approach have been proposed.[2–5] Some of them modify the image while preserving the topology, while others allow to selectively modify the topology in a controlled way. Applications to image filtering, segmentation and enhancement have been demonstrated. We present in this section some of these operators, which will be used in the next sections to illustrate our general method to reduce anisotropy.

4.1. Ultimate Thinning

Let $F \in \mathcal{F}$, $F' \in \mathcal{F}$. F' is a *lower (resp. upper) homotopic kernel* of F if F' is lower (resp. upper) homotopic to F, and if there is no destructible (resp. constructible) point for F'. In Fig. 1, (b) shows a lower homotopic kernel of (a) and (c) shows an upper homotopic kernel of (a).

A lower homotopic kernel of F can be obtained by successively selecting a destructible point x and lowering it down to $\delta^-(x, F)$. We repeat this operation until stability, i.e. until no more destructible point exists. Of course, different kernels can be obtained from the same image depending on the order in which destructible points are lowered. The Naive Ultimate Thinning algorithm below produces a lower homotopic kernel, also called an *ultimate skeleton*.

Algorithm 1: Naive Ultimate Thinning
Input: $F \in \mathcal{F}$
Output: F
(1) **repeat**
(2) select a destructible point x;
(3) $F(x) := \delta^-(x, F)$;
(4) **until** stability.

4.2. Curve Thinning

The Curve Thinning operator, as the Ultimate Thinning, preserves the cross-section topology. Furthermore, it better preserves the geometric information, especially for elongated crests. Let $X \subset \mathcal{Z}^2$ and $x \in X$, x is an *end point (for X)* if $\#(\Gamma_n^*(x) \cap X) = 1$. Let $F \in \mathcal{F}$ and $x \in \mathcal{Z}^2$, x is an *end point (for F)* if it is an end point for the set F_k with $k = F(x)$. The Curve Thinning algorithm lowers destructible points, as in the Ultimate Thinning algorithm, with exception of end points. The result of Curve Thinning is called a *curve skeleton*. Again, the order of selection of destructible points has an influence on the geometry of the skeleton.

Algorithm 2: Naive Curve Thinning
Input: $F \in \mathcal{F}$
Output: F
(1) **repeat**
(2) select a destructible point x;
(3) **if** x is a non-end point **then** $F(x) := \delta^-(x, F)$;
(4) **until** stability.

Figure 2(a-c) shows a typical application of Naive Ultimate Thinning and Naive Curve Thinning. We note that, for example, discrete curve segments of gray-level 9 have been preserved in (b), while the Naive Ultimate Thinning operator reduces the set of points of gray-level 9 to only one point. Ideally, we could expect a skeleton to be "thin" in the sense that the set of non-minimal regions contains no interior point. Unfortunately, it is not always the case: configurations like line crosses and others (see[2]) can produce thick non-minimal regions. This is the case in figure 2(d).

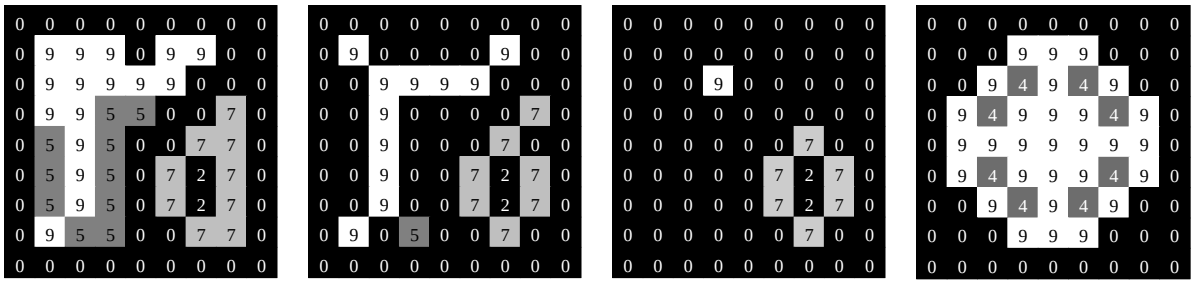

Figure 2. *Skeletons. (a): original image; (b): a curve skeleton of (a); (c): an ultimate skeleton of (a); (d): example of non-thin skeleton.*

4.3. Homotopic reconstruction

The homotopic reconstruction operator[4,5] is useful to recover the original values of certain pixels, after a topological modification. Let $F \in \mathcal{F}, G \in \mathcal{F}$ with $F \leq G$ (i.e., $\forall x \in \mathcal{Z}^2, F(x) \leq G(x)$), $F' \in \mathcal{F}$. F' is *homotopic to F under G* if $F' = F$ or if F' may be obtained from F by iteratively selecting a constructible point x such that the gray-level value of x is strictly lower than $G(x)$, and raising its gray-level value by 1. F' is an *(homotopic) reconstruction of F under G* if F' is homotopic to F under G and if there is no point $x \in \mathcal{Z}^2$ such that the value of x is strictly lower than $G(x)$, and x is constructible for F'. F is called a *marker* image. The dual notion of reconstruction of F over G is defined in an analogous way. In figure 3, we can see an example of reconstruction. We also show the corresponding result when using the well known reconstruction operator in the field of mathematical morphology (see[11] for example). Note that with the homotopic operator the reconstructed objects have the topology of the corresponding markers.

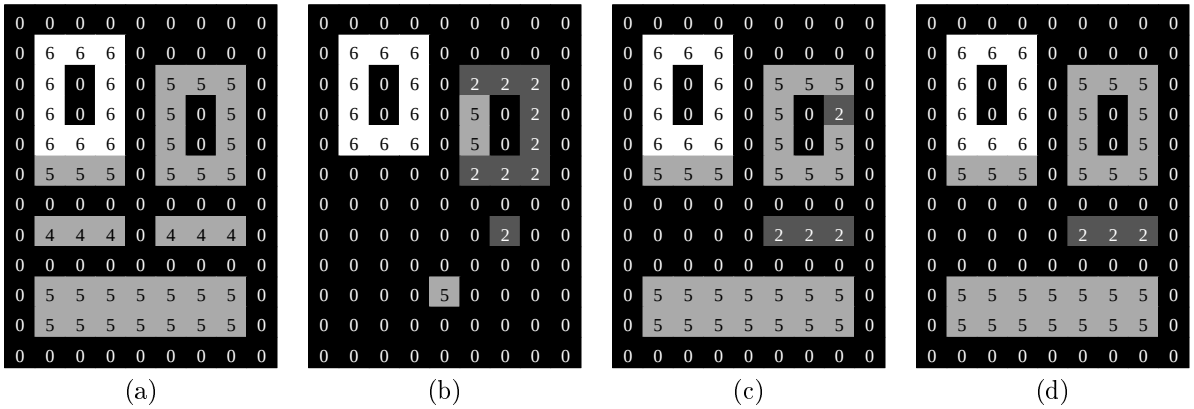

Figure 3. *Reconstruction. (a): original image; (b): marker image; (c): homotopic reconstruction of (b) under (a); (d): mathematical morphology reconstruction of (b) under (a).*

5. CENTERING

This section describes two algorithms found in literature providing centered skeletons and discuss their restrictions with respect to anisotropy.

The order of selection of destructible points in the algorithms Naive Ultimate Thinning and Naive Curve Thinning is important. Frequently, we need a kernel or skeleton to be well centered with respect to the initial object. We present below different approaches found in literature to achieve this goal. We remark that, with any of the algorithms presented in this article, we cannot obtain perfectly centered skeletons of, for example, even width lines because of the discrete nature of $\mathcal{Z}^2$. Thus, by centered skeleton we mean approximately centered skeleton. For a discussion on perfectly centered skeletons in the framework of orders, see Lohou and Bertrand.[12]

A well known curve thinning algorithm that produces nearly centered curve skeletons for binary images is based on a directional approach.[13] Let $X \subset \mathcal{Z}^2$. We say that a point $x \in X$ is a *north border point (for X)* if $(x_1+1,\, x_2) \in \overline{X}$; x is a *south border point* if $(x_1-1,\, x_2) \in \overline{X}$; x is an *east border point* if $(x_1,\, x_2+1) \in \overline{X}$; x is a *west border point* if $(x_1,\, x_2-1) \in \overline{X}$. This approach can be easily transposed to the case of grayscale images. Let $F \in \mathcal{F}$. A point $x \in \mathcal{Z}^2$ is a *north border point (for F)* if x is a north border point for F_k, with $k = F(x)$. The other border directional points for F are defined analogously. At each sub-iteration, the algorithm Directional Curve Thinning lowers down in parallel all non-end destructible border points in a given direction. In order to obtain centered curve skeletons, the considered direction is changed in successive sub-iterations, e.g. north-south-east-west.

We remark that this directional strategy cannot be used to obtain an homotopic kernel because components composed of only two destructible points with the same gray-level value could be lowered, thus changing the topology. As curve thinning doesn't lower down this type of point (they are both end points), topology preservation is assured for Directional Curve Thinning.

The Iterative Thinning algorithm[4,5] is better adapted for efficient implementation in non-parallel computers than Directional Curve Thinning. Furthermore, curve thinning can be done using the same approach. The thinning of $F \in \mathcal{F}$ is controlled using a list L of destructible points considered in the current iteration and an auxiliary image G where temporary gray-level values are stored. At each iteration, all destructible points are stored in L. Then, a point x is taken from L and, if it is still destructible for G, x is lowered down to the maximum between the values of $\delta^-(x,\, F)$ and $\delta^-(x,\, G)$. The image F stores the gray-level values of the previous iteration. The image G stores the gray-level values obtained in the current iteration. At the end of each iteration, we set $F := G$. Note that a point can be lowered several times during execution of this algorithm. Intuitively, the use of the list allows lowering the points by "layers".

Algorithm 3: Iterative Thinning
Input: $F \in \mathcal{F}$, $i \in \mathcal{N}$
Output: F
(1) $G := F$;
(2) **repeat** i times
(3) compute a list L of all destructible points;
(4) **foreach** x in L do
(5) **if** x is destructible for G **then** $G(x) := \max(\delta^-(x, G),\, \delta^-(x, F))$;
(6) $F := G$.

Iterative Thinning provides centered skeletons by controlling the propagation of the lowering process: the points are lowered in front waves or layers. If a point x is lowered down to a value k, then there exists a point $y \in F_k \setminus F_{k+1}$, i.e. $F(y) = k$, from which the gray-level value k has been propagated to x. At the first iteration, k can be propagated from y to, at most, the points in $\Gamma_8(y)$. We note that this is a breadth-first propagation: at each iteration the points that can be lowered down to k are 8-neighbors of a point lowered down to k in the previous iterations.

Obviously, this propagation is limited by the number i of applied iterations (see figure 5(a)). We can take advantage of this fact for controlling extent of the thinning: objects that have a width inferior to the parameter i can be completely thinned and can thus be detected and analyzed. Figures 4 and 6 exemplifies the anisotropy related to the application of Enhanced Thinning. We see in 4(b) that applying Iterative Thinning to the image (a) we change the original shape. Figure 4(c) shows a less anisotropic result that can be obtained by the method proposed in the next section.

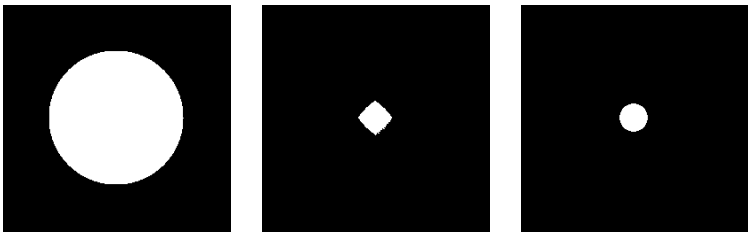

(a) (b) (c)

Figure 4. *Illustration of anisotropy. (a): original binary image; (b): result of Iterative Thinning; (c): result of Enhanced Thinning.*

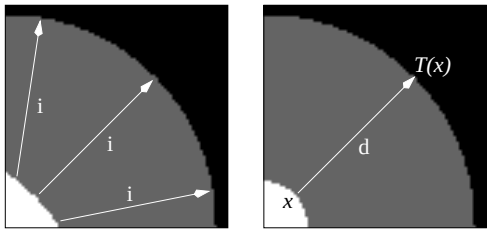

(a) (b)

Figure 5. *Anisotropy reduction. (a): result of Iterative Thinning on a part of image 4(a), after i steps. The zone in gray corresponds to the pixels, originally in white, that have been set to black during the process; (b): idem, using Enhanced Thinning, and a parameter value* $d_{max} = d$.

6. REDUCING ANISOTROPY

A common approach for generating centered skeletons of binary images uses distance maps. Let $X \subset \mathcal{Z}^2$ be a binary image. First we compute a distance map that, for each point $x \in X$ provides the distance from x to the background $\overline{X}$. Then, using the distance map, the centers of maximal disks inscribed in X are detected. A third step consists in linking the centers of maximal disks. This step is needed because the set of centers and X can have different topologies. The distance employed is the exact or approximate euclidean distance,[14] or more frequently the discrete distance d_4 or d_8. Another approach using distance maps consists of deletion of simple points in increasing distance of $\overline{X}$. Pudney[15] for example uses this approach for 3D images, using the chanfer distance, an integer approximation of the euclidean distance.

Also, a maximum distance parameter can be used in order to control the extent of the thinning, based on a width criterion. Suppose that we want to thin a grayscale image under the same kind of width constraint. Since we cannot build a distance map for a function, another method must be introduced. Our idea consists in limiting the propagation of the gray-level values with the help of pointers. To each point x we associate a pointer $T(x)$ that represents the spatial origin of the gray-level value $F(x)$ (see figure 5(b)). Initially, for each point x we set $T(x) := x$. These pointers will be updated during the thinning process using the strategy explained and discussed hereafter.

When a destructible point x is lowered down to a gray-level value k, it takes this value k from one of its neighbors. In order to limit the thinning, we must check that the distance between x and the spatial origin of k is not greater than the parameter d_{max}. On the other hand, among all the possible locations for the spatial origin of the value k, we want to consider only one that is nearest to x in order to thin the image as much as possible in the limit imposed by the width constraint. This problem is very similar to the problem of finding the Nearest Object Point (NOP) during the construction of an approximate or exact euclidean distance map. In the Danielsson's approach,[6] a simplifying assumption is made, which leads to a very simple linear algorithm giving a good approximation of the euclidean distance map. This assumption is the following: the relative location of the NOP for a point can be inferred from the location of the NOP of its n-neighbors (n=4 or n=8). In fact, this assumption isn't verified for certain configurations as pointed out by Cuisenaire,[8] who proposes a linear algorithm that builds an exact euclidean map. In our case, considering that the distance constraints have a lower priority than topological ones, we make the

same approximation as Danielsson in order to have a simpler algorithm.

When x is destructible and we execute the operation $F(x) := F(y)$, for some $y \in \Gamma_8(x)$, then the origin of x is updated to the origin of y, i.e. we also execute the operation $T(x) := T(y)$. This way, at any moment, $T(x)$ represents the location in the initial image of the origin of the current gray-level value of x. We can now use a distance measure between x and $T(y)$ to control the propagation of the gray-level values during the thinning process.

Let $d_e(x, y) = \sqrt{(x_1 - y_1)^2 + (x_2 - y_2)^2}$ be the euclidean distance between two points x and y of $\mathcal{Z}^2$. We define for a point $x \in \mathcal{Z}^2$:

$$\begin{aligned} \Delta(x) &= \{y \in \Gamma_8(x);\ F(y) = \delta^-(x, F)\}; \\ N(x) &= \text{a point } y \in \Delta(x) \text{ such that } d_e(x, T(y)) \text{ is minimal } ^*. \end{aligned}$$

Selecting y from $\Delta(x)$, we ensure topology preservation. At each iteration, we allow the lowering of a point x to $F(y)$ only if the distance $d_e(x, T(y))$ is not greater than the limit parameter d_{max}. Furthermore, we lower the points in increasing order of distance to the origin of the gray-level value. This strategy imposes the lowering of destructible points by layers, as in Iterative Thinning algorithm.

We present below Enhanced Thinning in algorithm 4. The parameter d_{max} controls the spatial extent of thinning. Using a sufficiently large distance d_{max}, we obtain an ultimate skeleton. Similarly, we can apply a variant of this method to obtain a curve skeleton.

In order to implement efficiently the algorithm 4, we need to store in L the quantity $d_e(x, N(x))$ together with each point x. The operations involved in steps (3) and (8) must be implemented efficiently. Line (8), the update of L involves the scanning of each point y in the 8-neighborhood of the point x. For each of these y, we must: i) delete y from L, if necessary; ii) check whether y is destructible or not; iii) and, if needed, store y in L together with $d_e(y, N(y))$. The basic operations in L can be executed in $O(n \lg n)$, n being the number of elements stored in L, if L is implemented as a balanced search tree, e.g. a RB-tree,[16] with the quantity $d_e(x, N(x))$ used as sorting key. Furthermore we need, for each image point x, a pointer to the location of the corresponding entry in L, to efficiently implement i).

Algorithm 4: Enhanced Thinning
Input: $F \in \mathcal{F}$, $d_{max} \in \mathcal{R}$
Output: F
(1) Let L be the set of all destructible points;
(2) **while** L is not empty
(3) select x in L such that $d_e(x, N(x))$ is minimal;
(4) remove x from L;
(5) **if** $d_e(x, N(x)) \leq d_{max}$
(6) $F(x) := F(N(x))$;
(7) $T(x) := T(N(x))$;
(8) update L;

In figure 4, (c) shows the result of application of Enhanced Thinning to image (a). We note that the circular shape is preserved. Figure 5 illustrates the differences between the application of Iterative Thinning and Enhanced Thinning to the disk of figure 4(a). The points in gray are those that have been lowered down. Figure 6 shows an example of an image with multiple gray-levels. We note that Enhanced Thinning (c) better preserves the round shape of the object extremities than Iterative Thinning (b).

7. APPLICATION: TOPOLOGICAL SEGMENTATION OF HEAD MRI

We present in this section an application to the segmentation of human head MRI images. The goal is to segment the layer extern to the bones of the head, which is composed by skin and muscles. In figure 7(a), the external layer consists of the elongated light ribbon in the superior part of the image. We remark that the image (figure 7(a)) has a particular anisotropy: the pixels have a rectangular shape due to the scanner parameters used for the

*This point may be arbitrarily chosen if several points satisfy these criteria. For soundness of the definition, we can state that it is the first one according to the scanning order.

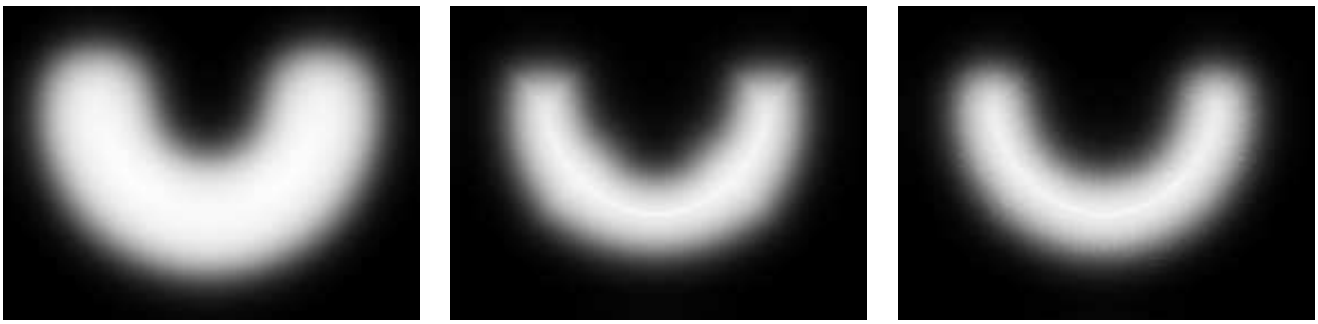

(a) (b) (c)

Figure 6. *Anisotropy reduction: an example with multiple gray-levels. (a): original image; (b): result of Iterative Thinning of (a); (c): result of Enhanced Thinning of (a).*

image capture. We know that the width of a pixel represents $1mm$ in the reality, and that the height of a pixel represents $1.35mm$. Thus, We will choose a distance measure better adapted to this situation than d_e. We define $d_{el}(x,\, y) = \sqrt{a^2(x_1 - y_1)^2 + b^2(x_2 - y_2)^2}$. Choosing $a = 1$ and $b = 1.35$, we can measure the actual euclidean distance, in mm, between two points in the head, corresponding to two given points in the image. For all topological operators used in this section we employ the distance d_{el}.

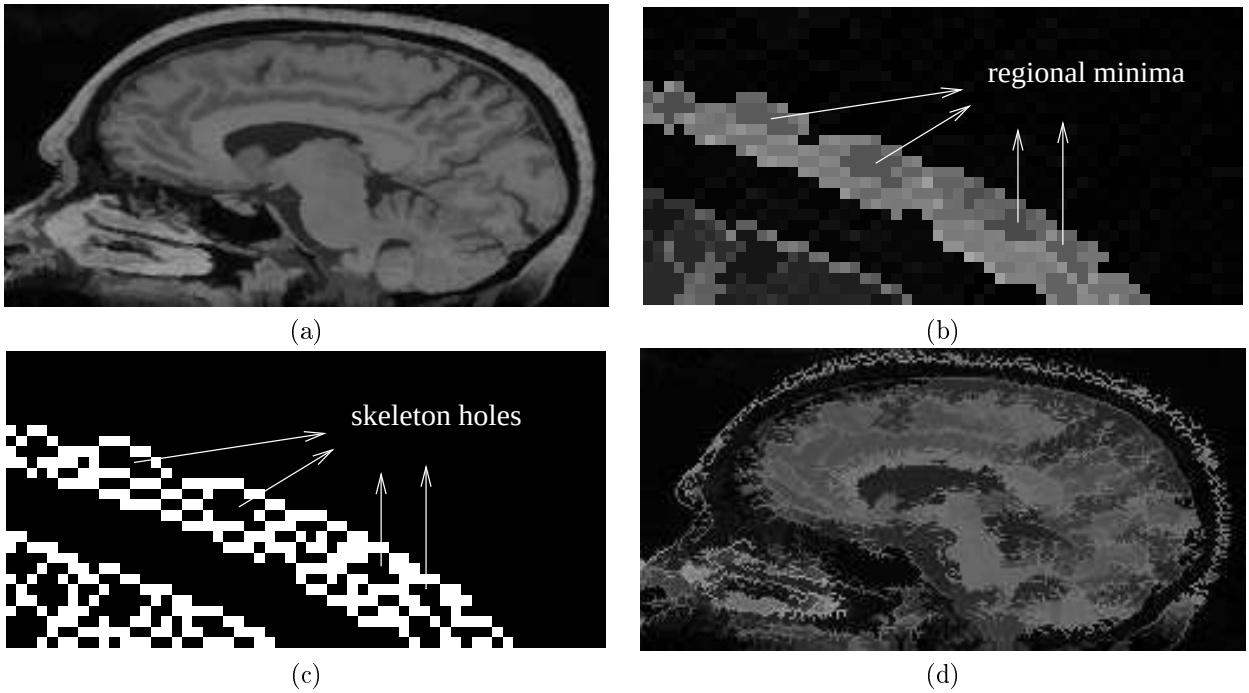

(a) (b) (c) (d)

Figure 7. *Segmentation of external layer of the head. (a): original human head MRI image; (b): some minima non-filtered thinned image; (c): skeleton holes corresponding to the minima in (c); (d): F', obtained after filtering and thinning of (a).*

Let us first sketch the whole method before describing each step in detail. We will find the marker corresponding to the structure to be segmented and proceed to an homotopic reconstruction. Due to the complexity of the image we need to consider some global characteristics of the layer we want to segment. Specifically, this layer is presented as a light (high gray-level values) ribbon with almost constant width crossing a large extension in the image. Our first idea is to apply Enhanced Thinning to the image, with the parameter d_{max} set to the approximated width of

the ribbon. We obtain a result that we call a (partial) skeleton. Then, we search in this skeleton for a large ridge (we will give later a precise definition of this notion) that has the same topology as the ribbon, i.e. a connected set without holes.

In fact, applying this approach directly to the image in figure 7(a), does not allow to find a suitable marker because the ribbon in (a) presents many small regional minima. Each of these minima corresponds to a hole in the set of ridge points of the skeleton, as shown in (c-d). Thus, a filtering procedure to eliminate small regional minima must be applied to (a) before thinning. We describe below this topologic filtering.[4,5]

7.1. Filtering

We can easily detect a minimum restricted to only one point: it is a well. A well x can be easily detected using topological numbers and can be eliminated by raising its gray-level value to $\alpha^+(x, F)$. We can filter out a larger minimum if we are able to reduce it to only one point.

Let $F \in \mathcal{F}$, $X \subset \mathcal{Z}^2$ a regional minimum of F that we want to eliminate. Suppose X is adjacent to only one component of $\overline{X}$, i.e. X has no hole. The points of gray-level 30 in figure 8(a) are an example of this case. In an homotopic kernel of F, the minimum corresponding to X is reduced to only one point. To better control the filtering, we introduce a parameter d_{max} that limits the size of the minima to be eliminated. We use the operator Enhanced Thickening which is the dual operator of Enhanced Thinning in order to reduce "small" minima to only one point. Then, once a minimum is reduced to only one point x, we set its gray-level value to $\alpha^+(x, F)$. Finally, we use topological reconstruction to restore the original gray-level values of those points that have been modified and that do not belong to small minima. In figure 8, (b-d) illustrate each step of the filter application for image (a). The points of gray-level 30 are set to gray-level 37.

Algorithm 5: Topological Filter
Input: $F \in \mathcal{F}$, $d_{max} \in \mathcal{R}$
Output: F
(1) $G := F$;
(2) $F :=$Enhanced Thickening(F, d_{max});
(3) **foreach** well x do $F(x) := \alpha^+(x, F)$;
(4) $F :=$homotopic reconstruction of F over G.

However, Topological Filter is unable to eliminate the minimum X composed by the points of gray-level 30 in figure 8(e) (consider $(n, \overline{n}) = (4, 8)$). The minimum X cannot be reduced to a well because of the point of gray-level 31: it is a peak that constitutes a hole in X. To eliminate a peak, or more generally, a small regional maximum of F, we can apply Topological Filter to $-F$. In this case, we must use the complementary connectedness $(\overline{n}, n)$, which is equal to (8,4) in the examples in figure 8. After the peak of gray-level 31 in (e) is eliminated, we have the same case as (a).

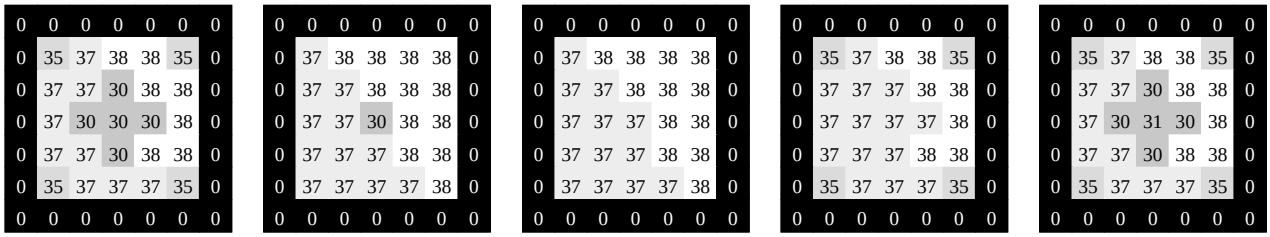

Figure 8. *Topological filter. (a): original image; (b): Thickening; (c): well elimination; (d): homotopic reconstruction; (e): the minimum at level 30 has a hole.*

7.2. Obtaining the marker

After the topological filtering, we can apply Enhanced Thinning to reduce the ribbon to a thin crest that will be used as marker. We call F' the image obtained after filtering and thinning. The next goal is to isolate the crest in

F' that corresponds to the ribbon among all the other crests. First, we need to precisely define the notion of thin crest, that we name *ridge*.

Let $X \subset \mathcal{Z}^2$ and $x \in X$, x is a *separating point (for X)* if $\overline{T}(x, X) \geq 2$. Let $F \in \mathcal{F}$, a point $x \in \mathcal{Z}^2$ is said to be a *separating point (for F)* if there exists $k \in \mathcal{Z}$ such that x is a separating point for the set F_k. A *ridge* is a maximal connected set of separating points.

In figure 10, (a) shows the set S constituted of separating points of F' (figure 7(d)). We note that the searched marker is a subset of S. So, we have to eliminate from S the crests not corresponding to the searched marker. Figure 9 represents schematically this situation. In (b), we can see the skeleton of the original image (a). The set S of separating points of (b) is shown in (c). In this example, a suitable marker would be the set composed of points of value 90 in (b). However, in S, these points are in the same component as the points of gray-level value 50. This is due to the minima adjacent to the ribbon in the original image. After thinning, the frontiers between these minima have been reduced to a set of separating points.

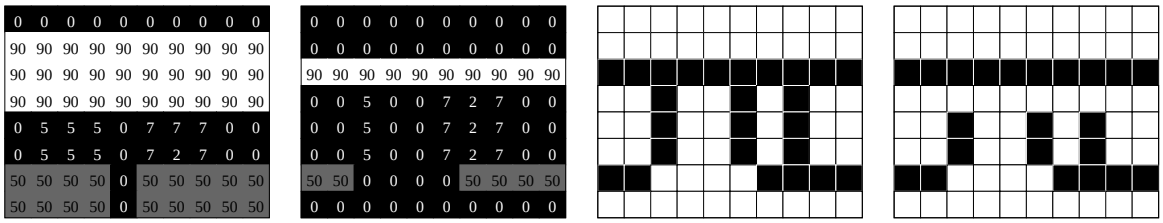

Figure 9. *Marker detection. (a): original image; (b): skeleton of (a); (c): separating points of (b); (d): 60-separating points of (b).*

In order to isolate the significant parts of the ridge, we introduce the notion of λ-separating point. Let $x \in \mathcal{Z}^2$ be a separating point for $F \in \mathcal{F}$ and $\lambda \in \mathcal{N}$. We say that x is a λ-*separating* point (for F) if $\Gamma^{++}(x, F) = \emptyset$ or if for all separating point $y \in \Gamma^{++}(x, F)$ we have $F(y) - F(x) \leq \lambda$. Intuitively, a λ-separating point is a separating point which does not have a much higher separating point in its neighborhood. We denote the set of λ-separating points of the image F' by S_λ. A λ-*ridge* is a maximal connected set of λ-separating points. Figure 9(d) shows the set S_{60} of (b). We observe that the points corresponding to gray-level 50 and the points corresponding to gray-level 90 in (b) are not in the same 60-ridges (d). Choosing a sufficiently high value of λ we are able to eliminate some separating points with low gray-level values, leading to a disconnection of the significant parts of the ridge set.

Now, we have to choose the correct component of S_λ as marker. Again, we exploit the global characteristics of the ribbon. As the ribbon has no holes, we eliminate all components of S_λ that are adjacent to more than one component of $\overline{S_\lambda}$. In figure 10, (b) shows the 60-ridges of F' that are without holes. As the ribbon has a large number of points, we take the larger remaining component of S_λ as marker (figure 10(c)). Once we have found a good marker, we simply apply reconstruction to recover the ribbon. The final result is shown in figure 10(d).

8. CONCLUSION

We presented a general method to reduce anisotropy of topological operators for grayscale images. It is based on the use of an approximation of the euclidean distance to control the thinning of a grayscale image. Furthermore, with limited distance values we can control the spatial extent of the thinning. This allows us to segment objects having a given width. We exemplify the method using the reduced anisotropy version of thinning, to build more complex filtering and segmentation operators. Specifically, we segment the external layer of the human head in MRI. The method allows us to choose a measure distance adapted to the anisotropy of the considered image.

REFERENCES

1. S. Beucher and F. Meyer. *Mathematical Morphology in Image Processing*, chapter The morphological approach to segmentation: the watershed transformation, Chap. 12, pages 433–481. Dougherty Ed., 1993.
2. G. Bertrand, J. C. Everat, and M. Couprie. Image segmentation through operators based upon topology. *Journal of Electronic Imaging*, 6(4):395–405, 1997.

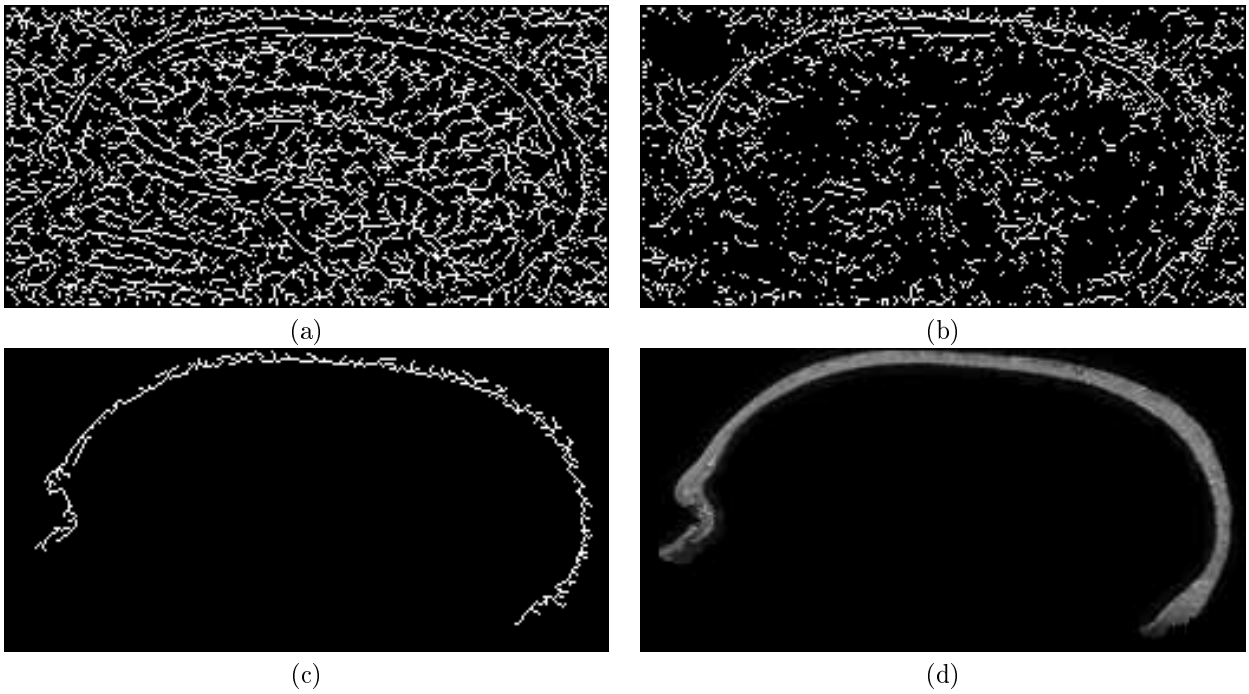

Figure 10. *(a): set of separating points of F'; (b): 60-ridges without holes; (c): largest component of without holes(marker); (d): external layer restored from marker.*

3. J.C. Everat. *Topologie des coupes et segmentation d'images par extraction de minima.* PhD thesis, Université Denis Diderot Paris VII, 1997.
4. M. Couprie, F. N. Bezerra, and G. Bertrand. Topological operators for grayscale image processing. *SPIE Vision Geometry VIII Proceedings*, 3168, 1999.
5. M. Couprie, F. N. Bezerra, and G. Bertrand. Grayscale image processing using topological operators. submitted to Journal of Electronic Imaging.
6. P. Danielsson. Euclidean distance mapping. *Computer Graphics and Image Processing*, 14:227–248, 1980.
7. G. Borgefors. Distance transformations in digital images. *Computer Vision Graphics Image Process.*, 34:344–371, 1986.
8. O. Cuisenaire and B. Macq. Fast euclidean distance transformation by propagation using multiple neighborhoods. *Computer Vision and Image Understanding*, 76(2):163–172, november 1999.
9. T.Y. Kong and A. Rosenfeld. Digital topology: introduction and survey. *Comp. Vision, Graphics and Image Proc.*, (48):357–393, 1989.
10. G. Bertrand. Simple points, topological numbers and geodesic neighborhoods in cubic grids. *Pattern Rec. Letters*, 15:1003–1011, 1994.
11. L. Vincent. Morphological grayscale reconstruction in image analysis: Applications and efficient algorithms. *IEEE Transactions on Image Processing*, 2(2), 1993.
12. C. Lohou and G. Bertrand. A new parallel thinning algorithm for 2d grayscale images. *SPIE Vision Geometry IX Proceedings*, 2000.
13. A. Rosenfeld and A. C. Kak. *Digital Image Proccessing.* Academic Press, second edition, 1982.
14. Y. G. and J. M. Fitzpatrick. On the generation of skeletons from discrete euclidean distance maps. *IEEE Transactions on PAMI*, 18(11):1055–1066, november 1996.
15. C. Pudney. Distance-ordered homotopic thinning: A skeletonization algorithm for 3d digital images. *Computer Vision and Image Understanding*, 72(3):404–413, december 1998.
16. C. Leiserson T. H. Cormen and R. Rivest. *Introduction to Algorithms.* McGraw-Hill, march 1990.
17. L. Lam, S. Lee, and C. Y. Suen. Thinning methodologies - A compreensive survey. *IEEE Transactions on PAMI*, 14:869–885, 1992.